Angular distributions of single pion charge exchange reactions to isobaric analog states in light nuclei

A. Doron, J. Alster, A. Erell, and M. A. Moinester
Department of Physics and Astronomy, Tel Aviv University, Ramat Aviv, Israel

R. A. Anderson, H. W. Baer, J. D. Bowman, M. D. Cooper, F. H. Cverna, C. M. Hoffman, N. S. P. King, M. J. Leitch, and J. P. Piffaretti*
The Clinton P. Anderson Meson Physics Facility, Los Alamos National Laboratory, Los Alamos, New Mexico 87545

C. D. Goodman
Department of Physics, Indiana University, Bloomington, Indiana 47401
(Received 8 January 1982)

Measurements of the angular distributions of the single charge exchange reactions to isobaric analog states for $^{13}C(\pi^+,\pi^0)^{13}N$ and $^{15}N(\pi^+,\pi^0)^{15}O$ at 165 MeV are described. The two angular distributions are very similar. The shapes are reproduced by semiphenomenological isobar-doorway calculations and by second-order coupled channels calculations. The calculated magnitudes are low by about a factor of 2. The measurements are consistent with older angle-integrated cross sections for ^{13}C.

[NUCLEAR REACTIONS ^{13}C, $^{15}N(\pi^+,\pi^0)$, $T_\pi=164$ MeV; measured $\sigma(\theta)$; IAS transitions; enriched targets; test of reaction models.]

I. INTRODUCTION

The pion-nucleus single charge exchange (SCE) reactions to isobaric analog states (IAS) have attracted much interest for many years. Although the charge exchange reactions represent only a small fraction of the total pion-nucleus cross section, they are important for our understanding of the pion-nucleus interaction. These reactions are governed by the isovector parts of the interaction, which, though they contribute to pion scattering, are not measurable directly by either elastic or inelastic scattering experiments. The expected simplicity of the reaction was not confirmed by experiments. Large disagreements between theories and available experimental data have persisted for several years.

Alster and Warszawski[1] reviewed the status of SCE reactions up to 1979. The measurement[2] of the reaction $^{13}C(\pi^+,\pi^0)$ ^{13}N(IAS) provided the first experimental excitation function for the SCE reaction to a single state. The angle-integrated cross sections were observed to be approximately 0.9 mb in the (3:3) resonance region. Most of the earlier theoretical activity was directed to the understanding of these data.[1] The first-order calculations predicted a deep minimum in the excitation function in the resonance region. The second-order calculations which were subsequently introduced did not improve the situation significantly even though the second order terms turned out to be large with respect to the first order terms. Higher order terms were introduced by means of various approximations. Different models for the πN off-shell extrapolation, the addition of two-nucleon correlation functions, and variations in the nuclear structure picture all produced effects of the same order of magnitude. In this paper we present the first angular distributions of pion SCE to IAS in nuclei. Since different angular distributions can add up to the same angle-integrated cross section, we expect the present data to provide new tests for the available theories and for those yet to come.

The present work is part of a systematic study of SCE reactions performed with the Clinton P. Anderson Meson Physics Facilty (LAMPF) π^0 spectrometer. Differential cross sections at forward angles have already been published, emphasizing various aspects of the reactions: the A dependence over a wide range of nuclei[3] at 100 MeV, small-angle cross sections for light nuclei at 165 MeV,[4] and small-angle excitation functions for ^7Li and ^{13}C.[5] An angular distribution of the SCE on ^3He has been

measured[6] as well.

In Sec. II we review the experimental procedures. Since most of the details have already been published,[7,8] we will review briefly the principle of operation and list the changes made since the detailed publication. Then we will discuss the data analysis in some detail. Results are presented in Sec. III together with a discussion of the most recent theories. Our conclusions are summarized in Sec. IV.

II. EXPERIMENTAL PROCEDURES

A. Data acquisition

The data were taken with the LAMPF π^0 spectrometer. Details of the design, construction, and initial performance are given in Refs. 7 and 8. The spectrometer detects the π^0's and measures their energies and directions by measuring the energies and directions of the two gamma rays from its main decay mode. The spectrometer consists of two position-sensitive detectors for high-energy gamma rays[9] (J arm and K arm). Each gamma ray can convert in one of three active Pb-glass converter planes (CNVP). Charged particles exiting the back of each converter are detected in three planes of multiwire proportional chambers (MWPC). One MWPC is in the scattering plane, while two others are perpendicular to it: Their information is used to determine the conversion point (CPT) of the gamma ray. The full electron shower is absorbed in an array of 15 Pb-glass blocks. The gamma ray energy is determined from the light output of the converters and the blocks. For each arm the line between the CPT and the target defines the gamma ray direction. Thus each arm measures independently the energy and direction of one photon. This information determines the energy and direction of the π^0 by the kinematical relation:

$$E_{\pi^0}{}^2=\frac{2m_{\pi^0}{}^2}{(1-\cos\eta)(1-X^2)} ,$$

where η is the angle between the two gammas and $X=(E_J-E_K)/(E_J+E_K)$, where $E_J(E_K)$ is the total γ energy measured in the J (K) arm. By limiting the data to events with small X, we can obtain good energy and angular resolution.

Following the performance tests reported in Ref. 7 some changes have been made to the spectrometer. We improved the trigger efficiency by increasing the thickness of the tagging plastic scintillators from 3 to 6 mm in order to improve the efficiency and light collection. The scintillator efficiencies were measured to be over 98% for the combined output from two photomultiplier (PM) tubes viewing each plate. New Pb-glass converters were used. Each converted plane was made of five strips, each 2.4 cm thick. This was done to allow higher instantaneous counting rates. Each strip was viewed by a photomultiplier tube, attached directly to the Pb-glass plate. Thus, the light collection was about 1.5 photoelectrons/MeV for the converters, the same as for the blocks. Light pulsers, made of ^{207}Bi embedded in plastic scintillators,[10] were put on each one of the Pb-glass elements to provide reference signals for gain stabilization of the PM tubes. The stabilization test was done about every 2 hrs. The gamma ray energy resolution was equivalent to 34% at 100 MeV. The MWPC efficiency was over 96% for each chamber.

The measurements were done at the low-energy pion channel at LAMPF. The pion flux was measured by an indirect method. The primary proton beam flux was measured during the experiments. For each channel setting the pion flux relative to the proton flux was determined by measuring the ^{11}C (β) activity[11] produced in thin scintillator disks. The accuracy of this technique is about 10%.

The ^{13}C target was made[12] of six self-supporting slabs, each 2.9 mm thick. Carbon powder enriched to 93% ^{13}C was bonded by furfuryl alcohol, pressed and baked. The final target had remnants of the bonding material of 6.4% by weight, thus reducing the ^{13}C enrichment to 87%. The density of the slabs was about 1 g/cm^3. The spectrometer has the desirable feature that the effect of energy loss in the target can be compensated by choosing an appropriate target density.[7,8] This allows the use of thick targets without loss of energy resolution. The desired average density of the target was set at each angle by adjusting the space between the six target slabs.

The ^{15}N was kept at nonboiling "liquid" temperatures inside a 1 cm thick, 7.6 cm$\times$14.0 cm cell, with 0.05 mm Mylar windows. The He gas was kept in pressure equilibrium with the ^{15}N vapors so that the thin windows would not bulge. The ^{15}N liquid density was 0.84 g/cm^3. The enrichment was 95%.

B. Data analysis

The hardware event trigger provided a necessary π^0 signature, but not of a quality sufficient for the

experiment. Many events that fulfilled the hardware event criteria were rejected subsequently in the data analysis by applying more stringent criteria in order to obtain better energy resolution. We will review the most important ones. We determined the current conversion plane in each arm by requiring that all three MWPC's following the active converter in that plane fire, but none in a preceding plane. In addition, a small energy deposition in the CNVP was required. A traceback algorithm was then used to determine the CPT. Only events with less than four lepton tracks exiting a converter and detected in a MWPC were accepted. The angle between the most forward track and the forward direction was limited in order to minimize the uncertainty introduced by multiple scattering in the Pb-glass converters.

The energy sharing parameter X is of special importance. The number of accepted events is approximately proportional to the maximum X allowed, so it is necessary to compromise resolution for efficiency. In the present analysis we included only events with $X < 0.15$. The typical energy resolution was 4 MeV FWHM and the typical angular resolution was 4 deg (FWHM).

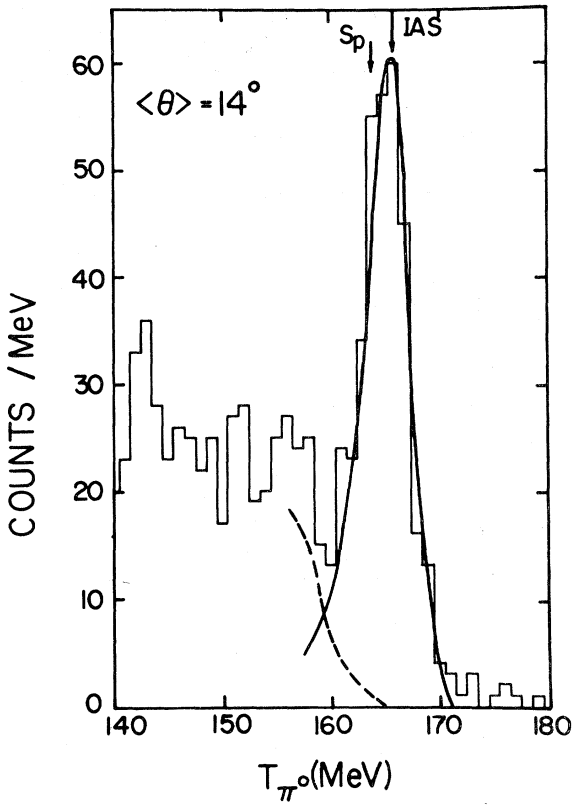

FIG. 1. Energy spectrum of π^0 from $^{13}C(\pi^+,\pi^0)^{13}N$ around 14 deg. The exponential tail of contributions from unbound states is shown by a dashed line. A solid line indicates the CH_2 line shape. Arrows denoted IAS and Sp indicate the energies corresponding to the IAS and to the separation threshold.

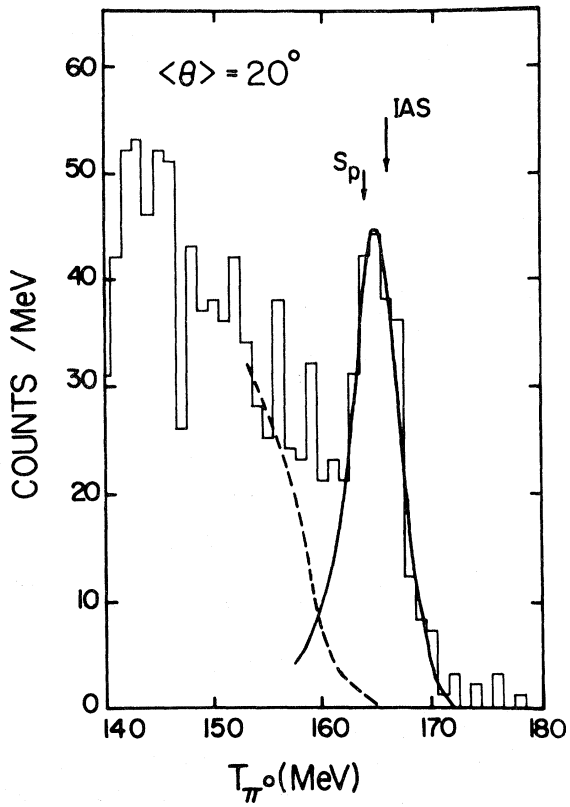

FIG. 2. Energy spectrum of π^0 from $^{13}C(\pi^+,\pi^0)^{13}N$ around 20 deg. See Fig. 1 for explanations.

The π^0 spectrometer has a wide angular acceptance of about 20 deg when set at a distance of 1.2 m from target to the first converter. We divided the events acquired in each spectrometer position (θ_0) into two or three angular bins, each larger than the angular resolution, but not necessarily of equal width. The ^{15}N cross sections were obtained from division into two bins, each 10 deg wide, around the central spectrometer position θ_0. The ^{13}C data were divided into three bins. The central bin was 5 deg wide around the central spectrometer position θ_0. The other two bins were 7.5 deg wide each.

Some of the spectra are shown in Figs. 1–6. We identified the IAS peak by its energy. Some contribution to the spectra was due to instrumental background, from either accidental π^0-like events or from reactions in the air behind the target. We assumed a linear background in the region of the IAS peak and fixed its magnitude and slope by the shape at π^0 energies above the ground state peak. At

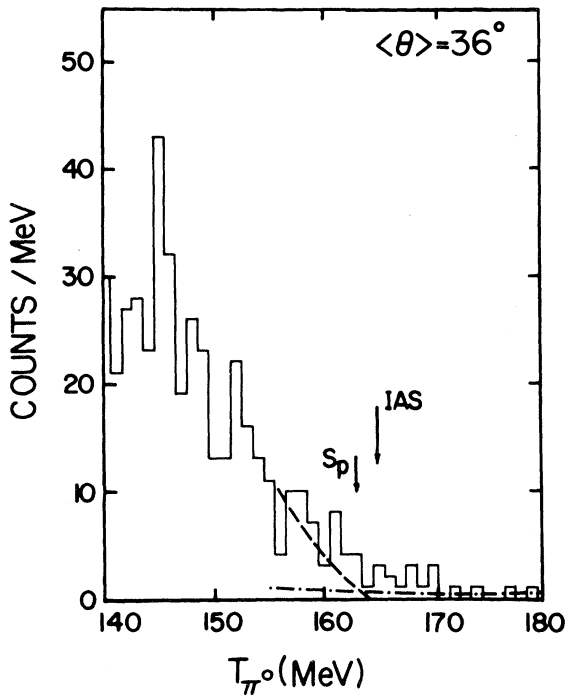

FIG. 3. Energy spectrum of π^0 from $^{13}C(\pi^+,\pi^0)^{13}N$ around 36 deg. See Fig. 1 for explanations. Note that this spectrum is in the region of the minimum in the angular distribution. Linear instrumental background is shown by a dotted dashed line.

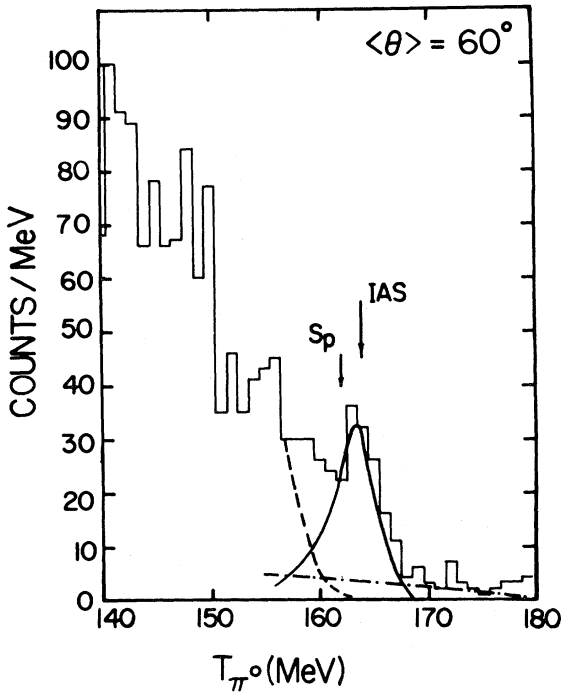

FIG. 4. Energy spectrum of π^0 from $^{13}C(\pi^+,\pi^0)^{13}N$ around 60 deg. See Fig. 1 for explanations. This spectrum is in the region of the second maximum of the angular distribution. Linear instrumental background is shown by a dotted dashed line.

lower π^0 energies, contributions to the spectra originate from excited nuclear states. The threshold of the continuum is indicated in the figures by an arrow, denoted by Sp. The tail of these contributions in the IAS peak region was obtained by exponential extrapolation (shown by dashed lines). The line shapes of the IAS peaks were similar to the line shapes obtained from the bombardment of CH_2 by π^-. The CH_2 line shapes are shown as solid lines.

The effective solid angles were determined as follows. The spectrometer was set at 20 deg and a CH_2 target was bombarded by π^-. The events were analyzed by the same criteria as the ^{13}C data. The same divisions in angular bins was used, and the $p(\pi^-,\pi^0)n$ peak areas were determined. Then we calculated the average cross sections for each angular bin using the phase shifts of Rowe *et al.*[13] and the angular distribution of the events. The ratios of the measured peak areas to the average $p(\pi^-,\pi^0)n$ cross sections determined the effective solid angles. Since the spectrometer efficiency is a function of π^0 energy, a correction had to be made to account for the energy difference between π^0's from $p(\pi^-,\pi^0)n$ and those from SCE on heavier nuclei. The effective solid angles for the other spectrometer angle

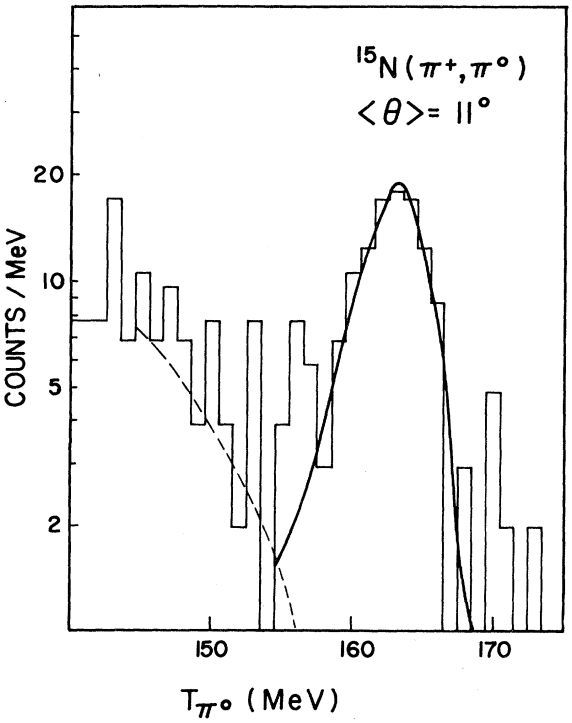

FIG. 5. Energy spectrum of π^0 from $^{15}N(\pi^+,\pi^0)^{15}O$ around 11 deg. See Fig. 1 for explanations.

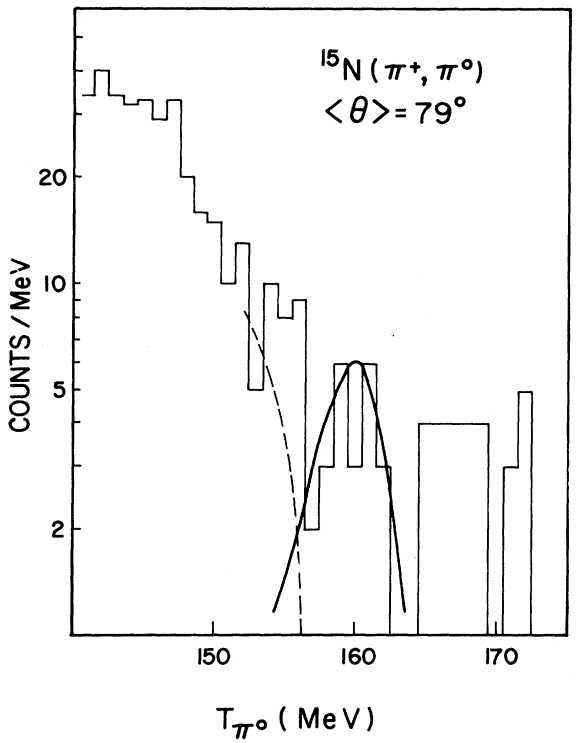

FIG. 6. Energy spectrum of π^0 from $^{15}N(\pi^+,\pi^0)^{15}O$ around 79 deg. See Fig. 1 for explanations.

settings were assumed to be the same (a good approximation).

The stability of the MWPC efficiencies influences the relative normalization. The efficiencies of the chambers were calculated for each run. The CNVP efficiencies E_i were calculated as the product of chamber efficiencies. The arm efficiencies were then defined as $(\sum_i N_i)/(\sum_i N_i/E_i)$, where N_i are the number of events which converted in the ith CNVP. The overall MWPC efficiency was then obtained by the product of the arm efficiencies; typically this was 85%.

Many effects contributed to the uncertainty of the measurements. The instrumental instability of the spectrometer, caused by small fluctuations in efficiencies and general performance, was estimated to be $\pm 5\%$. In addition, small differences in acceptance related to angle and energy measurements contributed about $\pm 4\%$. The relative errors included the unfolding uncertainty (including subtraction of instrumental background and of contributions from unbound states) and statistics. They varied from $\pm 5\%$ at forward angles to $\pm 40\%$ around the minima in the distributions. The absolute normalization error included uncertainties related to the ^{11}C production cross section (3%), the $p(\pi^-,\pi^0)n$ cross section (6%), the target thickness (3%), and corrections for photon attenuation in the target and surrounding material (6%). All these added, in quadrature, to $\pm 10\%$. The absolute normalization of the ^{15}N cross sections had an additional uncertainty of 5% due to an attenuation correction in the ^{15}N cryostat.

TABLE I. Angular distributions of (π^+,π^0) reactions at 165 MeV.

θ_0 deg[a]	θ deg[b]	$d\sigma/d\Omega$ mb/sr[c]
	$^{13}C(\pi^+,\pi^0)^{13}N$ (IAS)	
0	5	1.70 ±0.26
20	14	1.01 ±0.12
	20	0.65 ±0.07
	26	0.29 ±0.04
30	24	0.31 ±0.05
	30	0.10 +0.02−0.03
	36	0.07 +0.02−0.03
45	39	0.03 ±0.02
	45	0.06 ±0.01
	51	0.05 ±0.01
60	54	0.07 ±0.01
	60	0.050±0.008
	66	0.029±0.005
	$^{15}N(\pi^+,\pi^0)^{15}O$ (IAS)	
0	5	1.11 ±0.30
15	11	0.86 ±0.13
	19	0.60 ±0.10
30	26	0.27 ±0.05
	34	0.09 ±0.04
45	41	0.06 ±0.03
	49	0.09 ±0.03
60	56	0.07 ±0.01
	64	0.035±0.007
75	71	0.014±0.004
	79	0.010±0.003

[a]Angular position of the spectrometer.
[b]Central value of angular bin.
[c]Average cross section in angular bin. The errors quoted are relative.

III. RESULTS AND DISCUSSION

In Table I we present the measured cross sections. The angular distributions are drawn in Figs. 7 and 8. The data points are plotted at the mean angle in each angular bin. The vertical error bars represent the relative uncertainties only. The horizontal bars indicate the angular range corresponding to the bins used, as explained in the previous section.

The first excited state in $^{13}N(\frac{1}{2}^+)$ is at 2.37 MeV. Our energy resolution was not sufficient to separate this state from the IAS. Dehnhard *et al.*[14] and Schwarz *et al.*[15] showed that the analog of this state in ^{13}C at 3.09 MeV is very weakly excited by π^+ scattering. This state is very weakly excited in (p,n) (Ref. 16) reactions. Thus, the pion charge exchange to the first excited state can be expected to be weak. Also there is no experimental indication of much contribution from this state, which would appear as a widening of the peak. Transitions to higher lying states were taken into account by the background substraction.

In ^{15}O, there are two excited states, $\frac{1}{2}^+$ and $\frac{5}{2}^+$, near 5.2 MeV, easily separable from the IAS peak. They were barely seen in our spectra. The weakness of transitions to the $\frac{1}{2}^+$ state[17] corroborates our argument for neglecting contributions of transitions to the first excited state in ^{13}N.

Both ^{13}C and ^{15}N are p-shell nuclei with an excess of one neutron. Both ground states (g.s.) are $\frac{1}{2}^+$. In the simplest model the SCE reaction should be similar for the two targets and any differences should be due mainly to details in their nuclear structure. Indeed, the two distributions are quite similar, i.e., the first minimum in each distribution appears at nearly the same angle, at 38 ± 1 deg. For both nuclei, the second maxima are around 52 ± 2 deg and are of similar strength. We believe that the similarity of the angular distributions is a reflection of the same reaction mechanism for the two nuclei.

We now turn to a comparison of calculations for the ^{13}C angular distribution. The early calculations treated the SCE reaction as a direct process. Since large disagreements, up to a factor of 8, persisted between experiment and theory for the angle-integrated cross sections, many effects were added, under various approximations, in attempts to discover the main causes of the disagreements. It appeared that the various higher-order corrections contributed with similar strengths which, altogether, reduced the discrepancies to a factor of 2. Thus, it was concluded[1] that the addition of higher-order effects was not sufficient to reduce the exaggerated

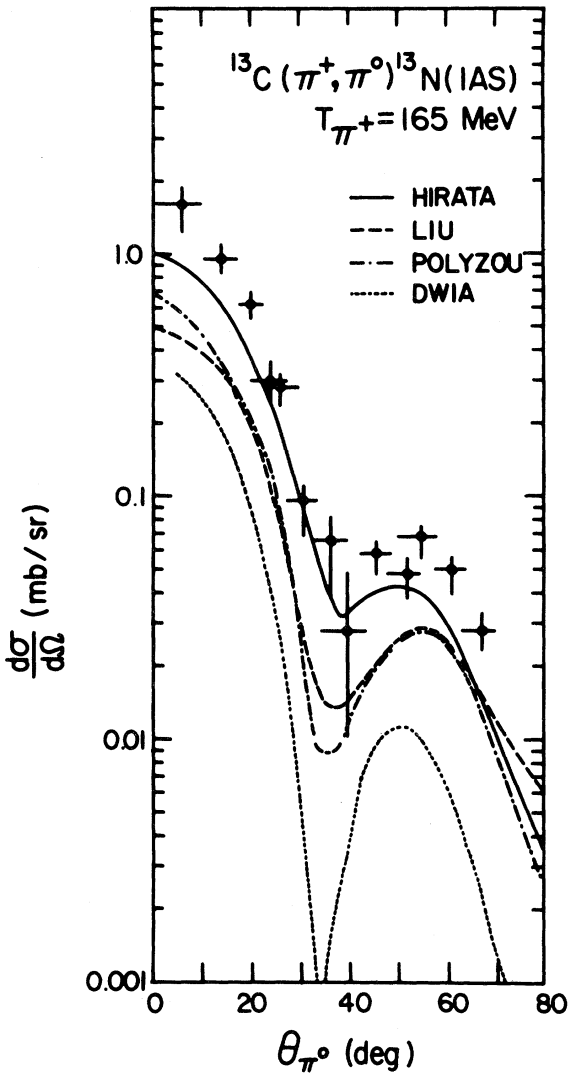

FIG. 7. Angular distribution of the reaction $^{13}C(\pi^+,\pi^0)^{13}N$ (IAS) at 165 MeV. Relative uncertainties are shown by vertical bars. The horizontal bars indicate the width of the angular bins corresponding to the data points. The solid curve is from the calculation of Hirata (Ref. 30). The dashed curve is from the calculation of Polyzou (Ref. 25). The dotted dashed curve is from the calculation of Liu (Ref. 22). The dotted line is our DWIA calculation. See text for details.

absorption contained in the first order DWIA calculations. We show a simple DWIA angular distribution, shown as a dotted line in Figs. 7 and 8, to represent the main discrepancies with a large class of multiple scattering theories which were not compared previously to angular distributions. Our calculation was done with a modified version of DWPI.[18] A simple Kisslinger potential was used with potential parameters derived from the phase

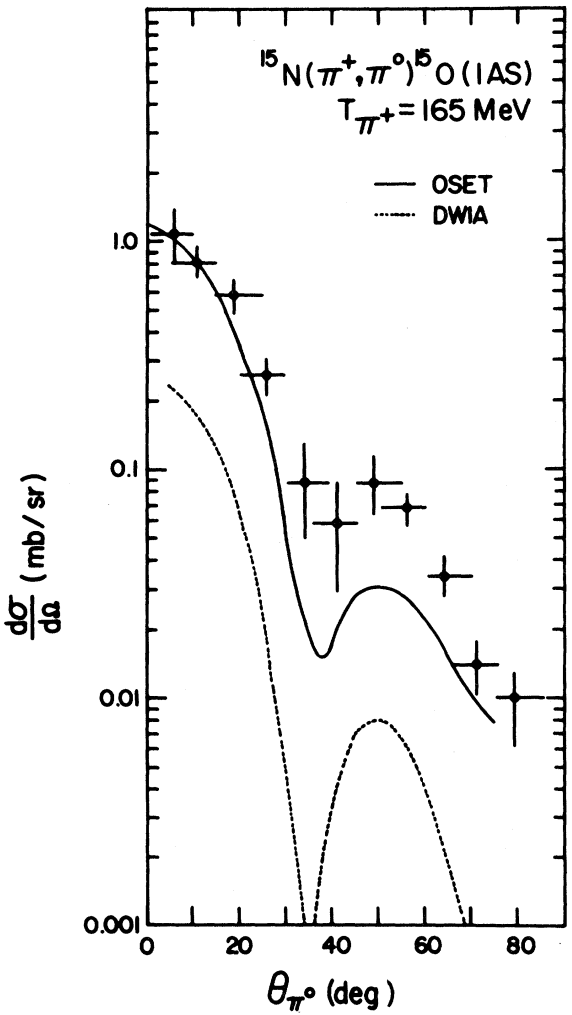

FIG. 8. Angular distribution of the reaction $^{15}N(\pi^+,\pi^0)^{15}O$ (IAS) at 165 MeV. See Fig. 7 for explanation of the data points. The solid line is from the calculation of Oset (Ref. 31). The dotted line is our DWIA calculation.

shifts of Rowe *et al.*[13] Such calculations are known to have a dip in the excitation function in the resonance region, the calculated angle-integrated cross section being too low by a factor of 8. The slope of the theoretical distribution is too steep, resulting in a deep minimum at too small an angle. Furthermore, the second maximum is too low by a factor of 5. It is interesting to note that the angular distribution calculated using π-N phase shifts at 136 MeV has a shape very similar to the experimental one at 165 MeV but it is still too low in magnitude by a factor of 6. This was also observed in elastic scattering for a variety of nuclei,[19] and was assumed to express the effect of the Fermi motion of the nucleons. Thus, some of the effects missing in the simple DWIA could be mocked up by a drastic reduction in the effective interaction energy, which cannot be justified by kinematical factors.

The conclusion that the first-order DWIA calculations contain too much absorption had already been reached[1] on the basis of the disagreement with the overall magnitude of the cross sections. Presently, the DWIA analysis of the shape of the angular distribution provides an additional and independent indication of the same effect. The minimum in the DWIA occurs at an angle that is too small by approximately 5 deg, which corresponds to an interaction radius that is too large by approximately 0.3 fm. Indeed, artificially reducing the absorption in the calculation by a factor of 2 moves the minimum to the correct position. It does not raise the magnitude of the cross section sufficiently, however.

Chakravarti[20] has performed coupled-channel calculations using shell-model wave functions of Cohen and Kurath.[21] True pion absorption was included phenomenologically by adjusting the radius parameter of the density to fit elastic scattering. He has found that the coupling of the $\frac{3}{2}^-$ and $\frac{5}{2}^-$ states in ^{13}C, which are strongly excited by inelastic pion scattering, effects significantly the angle-integrated cross section with only minor modifications in the shape of the angular distribution. Still, his cross sections are too low (a factor of 2 at small angles) and miss the minimum by 20 deg.

Liu[22] has recently published a coupled-channel calculation in which second-order effects were included consistently in the transition and in the distortions. He used a complex energy-dependent pion-nucleus potential derived from unitarity considerations. The presence of the product of the πN scattering amplitude with its complex conjugate represents the main difference between his approach and the usual multiple-scattering calculation of the second-order optical potential. The angular distribution obtained from his calculation is drawn by a dashed line in Fig. 7. The shape of the distribution is very similar to the experiment but is too low by a factor of 3.

Some recent theories calculate the SCE reaction emphasizing the difference between the amplitudes in the two isospin channels. Saharia and Woloshyn[23] were able to fit the angle-integrated SCE cross section as a function of energy, but took a purely phenomenological energy dependence of the energy difference between the amplitudes. Landau and Thomas[24] obtained the same results with a small and constant energy shift by using a better

optical potential. In a previous publication[5] we have shown that their calculations agree well with the small-angle excitation functions. In the present work we find that the full angular distribution disagrees with the experiment.

Polyzou *et al.*[25] have recently published a calculation in which energy shift between the isospin amplitudes is derived[26] based on the fractional parentage expansion of the nuclear states, as suggested by Moniz and Toyama.[27] Spectroscopic factors and core energies were taken from Cohen and Kurath.[21] A Kisslinger form potential was used with a separable off-shell extrapolation with a cutoff at 600 MeV. The potential parameters were obtained from a fit to ^{12}C elastic scattering. The effect of the energy shift was shown to be only 20% and did not affect the shape of the distribution. The angular distribution shape, shown in Fig. 7 by a dotted-dashed line, resembles the experimental one, but for an overall normalization factor of 2.

Recently, several isobar-doorway model calculations[27-30] have been published. This approach is partially phenomenological because it needs fits to elastic scattering in order to fix some of the parameters in the calculations. It has the advantage that it automatically includes many higher order effects. Hirata[30] has calculated the angular distributions in this approach. He included recoil and binding energy corrections to the pion-nucleus amplitudes. Pauli-quenching effects in the decay of the delta and its spreading potential were taken into account. Particle hole and isobar wave functions are described by harmonic oscillator wave functions. Hirata obtained an excitation function for the angle-integrated cross section which is flat but too low by a factor of 2. The angular distribution predicted by his calculation is shown by a solid line in Fig. 7. The shape agrees with the experimental distribution but disagrees in magnitude by a factor of 2.

A similar calculation has been done by Oset[31] for the SCE on ^{15}N. His isobar-hole calculation takes into account effects of antisymmetry, true pion absorption, and other rescattering terms. The resulting angular distribution is shown by a solid line in Fig. 8. The agreement is good at the small angles but fails at the second maximum. It thus appears that the discrepancy of a factor of about 2 is not a feature of ^{13}C alone.

For historical reasons it is interesting to perform an integration of the experimental angular distribution to compare to the older ^{13}C data.[2] The angle-integrated cross section was[2] 0.92 ± 0.14 mb. The integral of our distribution up to 60 deg yields 0.72 ± 0.18 mb: some contributions to the integral from larger angles have yet to be added. This result is consistent with the older measurement.

IV. CONCLUSIONS

First-order DWIA calculations disagree in magnitude and shape with the angular distributions. Both discrepancies point towards a surplus of absorption in the DWIA. The angular distributions for the SCE reactions on ^{13}C and ^{15}N are similar. The shape of the angular distributions can be reproduced by phenomenological isobar-hole calculations and by second-order coupled-channel calculations. Discrepancies of a factor of 2 in magnitude still remain between the most successful calculations and the experimental results. The new measurement of the angular distribution of the reaction $^{13}C(\pi^+,\pi^0)^{13}N$ (IAS) is consistent with the previously measured angle-integrated cross section. Clearly, more theoretical effort is needed to understand these results.

Note added in proof. A very recent private communication from Saharia shows that their calculation gives good agreement for ^{13}C but is 50% too high at small angles for ^{15}N.

ACKNOWLEDGMENTS

We wish to express our appreciation to many people whose efforts made this work possible: R. Bolton, R. Damjanovich, J. Harrison, M. Oothoudt, J. Novak, J. Sandoval, J. Sena, H. Schoenberg, J. Simms, and R. Werbeck at LAMPF. We acknowledge useful discussions with Dr. N. Auerbach, Dr. J. Eisenberg, Dr. A. Gal, Dr. W. Gibbs, Dr. M. Johnson, Dr. E. Siciliano, and Dr. J. Warszawski. We thank Dr. Oset and Dr. Hirata for sending us their calculations prior to publication. This work was supported in part by the U. S. Department of Energy and by the U. S.-Israel Binational Science Foundation, Jerusalem, Israel.

*Permanent address: Schweizerisches Institut für Nuklearforschung, Villigen Switzerland.

[1]J. Alster and J. Warszawski, Phys. Rep. 52, 87 (1979), and references within.

[2]Y. Shamai, J. Alster, D. Ashery, S. Cochavi, M. A. Moinester, A. I. Yavin, E. D. Arthur, and D. M. Drake, Phys. Rev. Lett. 36, 82 (1976).

[3]H. W. Baer, J. D. Bowman, M. D. Cooper, F. H. Cverna, C. M. Hoffman, M. B. Johnson, N. S. P. King, E. R. Siciliano, J. Piffaretti, J. Alster, A. Doron, S. Gilad, M. A. Moinester, P. R. Bevington, and E. Winkelmann, Phys. Rev. Lett. 45, 982 (1980).

[4]A. Doron, J. Alster, A. Erell, S. Gilad, M. A. Moinester, H. W. Baer, J. D. Bowman, M. D. Cooper, F. H. Cverna, C. M. Hoffman, M. B. Johnson, N. S. P. King, J. Piffaretti, P. R. Bevington, E. Winkelmann, and C. D. Goodman, Phys. Rev. C (to be published).

[5]A. Doron, J. Alster, A. Erell, S. Gilad, M. A. Moinester, H. W. Baer, J. D. Bowman, M. D. Cooper, F. H. Cverna, C. M. Hoffman, M. B. Johnson, N. S. P. King, J. Piffaretti, and P. R. Bevington, Phys. Rev. Lett. 48, 989 (1982).

[6]M. D. Cooper, H. W. Baer, J. D. Bowman, F. H. Cverna, R. H. Heffner, C. M. Hoffman, N. S. P. King, J. Piffaretti, J. Alster, A. Doron, S. Gilad, M. A. Moinester, P. R. Bevington, and E. Winkelmann, Phys. Rev. C 25, 438 (1982).

[7]H. W. Baer, R. D. Bolton, J. D. Bowman, M. D. Cooper, F. H. Cverna, C. M. Hoffman, N. S. P. King, J. Piffaretti, J. Alster, A. Doron, S. Gilad, M. A. Moinester, P. R. Bevington, and E. Winkelmann, Nucl. Instrum. Methods 180, 445 (1981).

[8]S. Gilad, Ph. D. thesis, Tel-Aviv University, 1979 (unpublished).

[9]S. Gilad, J. D. Bowman, M. D. Cooper, D. M. Hoffman, M. A. Moinester, J. M. Potter, R. H. Heffner, F. H. Cverna, H. W. Baer, P. R. Bevington, and M. W. McNaughton, Nucl. Instrum. Methods 144, 103 (1977).

[10]R. D. Bolton, H. W. Baer, J. D. Bowman, and L. Gordon, Nucl. Instrum. Methods 174, 411 (1980).

[11]B. J. Dropesky, G. W. Butler, C. J. Orth, R. A. Williams, M. A. Yates-Williams, G. Friedlander, and S. B. Kauffman, Phys. Rev. C 20, 1844 (1979).

[12]Produced by H. Schoenberg at Los Alamos National Laboratory.

[13]G. Rowe, M. Salomon, and R. H. Landau, Phys. Rev. C 18, 584 (1978).

[14]D. Dehnhard, S. J. Tripp, M. A. Franey, G. S. Kyle, C. L. Morris, R. L. Boudrie, J. Piffaretti, and H. A. Thiessen, Phys. Rev. Lett. 43, 1091 (1979).

[15]E. Schwarz, J. P. Egger, F. Goetz, P. Gretillat, C. Lunke, C. Perrin, B. M. Preedom, and R. E. Mischke, Phys. Rev. Lett. 43, 1578 (1979).

[16]A. S. Clough, C. J. Batty, B. E. Bonner, and L. E. Williams, Nucl. Phys. A143, 385 (1970).

[17]T.-S. H. Lee and D. Kurath, Phys. Rev. C 22, 1670 (1980).

[18]R. A. Eisenstein and G. A. Miller, Comput. Phys. Commun. 11, 95 (1976).

[19]W. B. Cottingame and D. B. Holtkamp, Phys. Rev. Lett. 45, 1828 (1980).

[20]S. Chakravarti, Phys. Lett. 90B, 350 (1980).

[21]S. Cohen and D. Kurath, Nucl. Phys. A101, 1 (1967).

[22]L. C. Liu, Phys. Rev. C 23, 814 (1981).

[23]A. Saharia and R. M. Woloshyn, Phys. Lett. 84B, 401 (1979).

[24]R. H. Landau and A. W. Thomas, Phys. Lett. 88B, 226 (1979).

[25]W. N. Polyzou, W. R. Gibbs, and G. J. Stephenson, Phys. Rev. C 23, 2648 (1981).

[26]A. Gal (private communication).

[27]E. J. Moniz, in *Proceedings of the International Conference on Nuclear Physics with Electromagnetic Interactions, Mainz, 1979* (Springer, Berlin, 1979), p. 435.

[28]N. Auerbach, Phys. Rev. Lett. 38, 804 (1977).

[29]A. N. Saharia and R. M. Woloshyn, Phys. Rev. C 21, 1111 (1980).

[30]M. Hirata, Phys. Rev. C 24, 1604 (1981).

[31]E. Oset, Nucl. Phys. A356, 413 (1981).